Received: 4 October 2021 | Revised: 18 December 2021 | Accepted: 21 December 2021 | Published online: 1 March 2022

DOI: 10.1002/trc2.12258

Alzheimer's & Dementia
Translational Research & Clinical Interventions

RESEARCH ARTICLE

Exploratory imaging outcomes of a phase 1b/2a clinical trial of allopregnanolone as a regenerative therapeutic for Alzheimer's disease: Structural effects and functional connectivity outcomes

Adam C. Raikes[1] | **Gerson D. Hernandez**[1] | **Dawn C. Matthews**[2] | **Ana S. Lukic**[2] | **Meng Law**[3] | **Yonggang Shi**[4] | **Lon S. Schneider**[5] | **Roberta D. Brinton**[1]

[1] Center for Innovation in Brain Science, University of Arizona, Tucson, Arizona, USA

[2] Departments of Pharmacology and Neurology, College of Medicine, ADM Diagnostics, Northbrook, Illinois, USA

[3] Department of Radiology, Alfred Health, Department of Neuroscience and Computer Systems Engineering, Monash University, Melbourne, Australia

[4] Stevens Neuroimaging and Informatics Institute, Keck School of Medicine, University of Southern California, Los Angeles, California, USA

[5] Keck School of Medicine, University of Southern California, Los Angeles, California, USA

Correspondence
Roberta Diaz Brinton, Center for Innovation in Brain Science, University of Arizona, 1230 N. Cherry Ave, PO Box 210242, Tucson, AZ 85721-0242, USA.
Email: rbrinton@arizona.edu

Funding information
National Institute on Aging, Grant/Award Numbers: UF-1AG046148, U01-AG031115, U01-AG047222; USC ADRC clinical core, Grant/Award Numbers: ADDF-20150701, P30-AG066530

Abstract

Introduction: Allopregnanolone (ALLO), an endogenous neurosteroid, promoted neurogenesis and oligogenesis and restored cognitive function in animal models of Alzheimer's disease (AD). Based on these discovery research findings, we conducted a randomized-controlled phase 1b/2a multiple ascending dose trial of ALLO in persons with early AD (NCT02221622) to assess safety, tolerability, and pharmacokinetics. Exploratory imaging outcomes to determine whether ALLO impacted hippocampal structure, white matter integrity, and functional connectivity are reported.

Methods: Twenty-four individuals participated in the trial ($n = 6$ placebo; $n = 18$ ALLO) and underwent brain magnetic resonance imaging (MRI) before and after 12 weeks of treatment. Hippocampal atrophy rate was determined from volumetric MRI, computed as rate of change, and qualitatively assessed between ALLO and placebo sex, apolipoprotein E (*APOE*) ε4 allele, and ALLO dose subgroups. White matter microstructural integrity was compared between placebo and ALLO using fractional and quantitative anisotropy (QA). Changes in local, inter-regional, and network-level functional connectivity were also compared between groups using resting-state functional MRI.

Results: Rate of decline in hippocampal volume was slowed, and in some cases reversed, in the ALLO group compared to placebo. Gain of hippocampal volume was evident in *APOE* ε4 carriers (range: 0.6% to 7.8% increased hippocampal volume). Multiple measures of white matter integrity indicated evidence of preserved or improved integrity. ALLO significantly increased fractional anisotropy (FA) in 690 of 690 and QA in 1416 of 1888 fiber tracts, located primarily in the corpus callosum, bilateral thalamic radiations, and bilateral corticospinal tracts. Consistent with structural changes, ALLO strengthened local, inter-regional, and network level functional connectivity in

AD-vulnerable regions, including the precuneus and posterior cingulate, and network connections between the default mode network and limbic system.

Discussion: Indicators of regeneration from previous preclinical studies and these exploratory MRI-based outcomes from this phase 1b/2a clinical cohort support advancement to a phase 2 proof-of-concept efficacy clinical trial of ALLO as a regenerative therapeutic for mild AD (REGEN-BRAIN study; NCT04838301).

KEYWORDS
allopregnanolone, Alzheimer's disease, functional connectivity, hippocampal volume, regenerative therapeutic, white matter integrity

1 | BACKGROUND

Alzheimer's disease (AD) is a progressive neurodegenerative disease currently affecting 6.2 million people in the United States.[1] Therapies to effectively treat AD by targeting underlying mechanisms remain an unmet need.[2] Because brain atrophy is an early indicator of AD, is correlated with cognitive decline, and progresses throughout the course of the disease, therapeutics targeting regeneration of brain structure have the potential to restore associated brain function.[3] A substantial body of research indicates that allopregnanolone (ALLO) promotes neurogenesis, restores cognitive function, and reduces AD pathology in preclinical AD models.[4–10]

ALLO is a small molecular weight, blood-brain barrier penetrant molecule that promotes neurogenesis through regeneration of neural stem cells in brain[4–8] and promotes the brain's innate regenerative capacity to increase the pool of neural progenitor cells[3,5,7,8] and their differentiation to neurons.[8] Clinical development of ALLO is supported by abundant US Food and Drug Administration Investigation New Applications (FDA-INDs) enabling safety data in animals and humans.[11–15]

Recently a phase 1b/2a randomized, double-blinded, placebo-controlled, single and multiple ascending dose trial of ALLO was conducted in persons with early AD (mild cognitive impairment due to AD or mild AD) (NCT02221622).[12] Primary outcome analyses indicated that ALLO was safe and well-tolerated across all doses.[12] Safety, maximally tolerated dose (MTD), and pharmacokinetics (PK) profiles supported advancement of ALLO as a regenerative therapeutic for AD to a phase 2 efficacy trial (NCT04838301). Here we report exploratory imaging outcomes from that phase 1b/2a clinical trial of ALLO.

Imaging biomarkers are well-documented indicators of neurodegeneration and are used for AD staging severity.[16–20] Whole brain and hippocampal atrophy on magnetic resonance imaging (MRI) are the most consistently used biomarkers for diagnosis and assessment of disease progression in AD.[16,17,20,21] The FDA and European Medicines Agency (EMA) have validated and accepted hippocampal atrophy rate as suitable for aiding in the design of clinical trials in patients with mild to moderate AD.[22,23]

Diffusion-weighted imaging (DWI) and resting state functional MRI (rs-fMRI) provide information regarding microstructural integrity, brain function, and connectivity that can serve as potential target engagement markers of regeneration.[24,25] Previous studies demonstrate that connectivity and network integrity decline is markedly accelerated in AD, particularly within the default mode network (DMN).[26–28] Measures of functional connectivity have been proposed as promising biomarkers for interventional trials given the correlation with cognitive improvement following treatment.[29,30]

The primary purpose of these analyses was to investigate exploratory endpoints from the phase 1b/2a ALLO clinical trial.[12] Rate of hippocampal atrophy, white matter integrity, and functional connectivity were specifically investigated to inform future ALLO clinical trials for the treatment of AD. Outcomes described herein served as the foundation for the design of a phase 2 clinical trial of ALLO as a neuro-regenerative therapeutic for AD.

2 | METHODS

2.1 | Trial design

The phase 1b/2a trial was a single-site, randomized, double-blinded, placebo-controlled, multiple ascending dose study of 12-weeks duration in persons with early AD. Eligibility, recruitment, and trial design for this study have been described previously.[12] Participants were randomized into three dosing cohorts of ALLO (2 mg, 4 mg, and 6–18 mg) or placebo at a 6:2 allocation ratio. The third cohort underwent multiple ascending dosing. The treatment regimen consisted of a 30-minute intravenous infusion once-per-week. A total of 24 participants (mean age ± SD: 75.88 ± 7.17, range: 60–89) were enrolled into the trial and underwent safety, pharmacokinetic, cognitive, and imaging assessments. All participants had a Mini Mental Status Examination (MMSE) score between 20 and 26 and were in general good health and known co-morbidities were stable. Most participants ($n = 21$) were taking more than one concomitant medication, including supplements. All participants taking concomitant medications had stable dosing for at least 3 months prior to enrollment. Use of benzodiazepines, sedatives/hypnotics, anticonvulsants, antipsychotics, and other medications that might interact with the γ-aminobutyric acid $(GABA)_A$ receptor complex were not allowed. The study was approved by the FDA and

TABLE 1 Demographic characteristics of individuals included in imaging analyses

	ALLO $n = 18$	Placebo $n = 6$	*P*-value
Age (years)	74.1 ± 7.2	81.3 ± 3.3	.028[b]
Sex: *Female/Male (n)*	9/9	3/3	1[c]
APOE genotype[a]: *APOE* $^{e4+}$/*APOE* $^{e3/e3}$ *(n)*	13/5	2/4	.224[c]
Years of education	15.7 ± 2.6	15.5 ± 2.2	.851[b]
MMSE total score	24.0 ± 2.0	23.5 ± 4.0	.781[b]
MoCA total score	20.2 ± 3.1	18.0 ± 6.3	.449[b]
ADAScog14 total score	24.8 ± 8.4	26.7 ± 12.0	.673[b]
GDS total score	1.8 ± 1.3	1.8 ± 2.2	1[b]
FAQ total score	8.6 ± 8.5	8.2 ± 7.4	.91[b]

Notes:
All values are reported as mean ± standard deviation or *n*/*n*.
Abbreviations: ADAS: Alzheimer's Disease Assessment Scale; FAQ: Functional Activities Questionnaire.; GDS: Geriatric Depression Scale; MMSE: Mini Mental Status Examination;
MoCA: Montreal Cognitive Assessment.
[a]*APOE* $^{e4+}$ includes *APOE* $^{e3/e4}$ and *APOE* $^{e4/e4}$ individuals.
[b]Two-sample *t*-test.
[c]Chi-square test.

the University of Southern California (USC) Institutional Review Board and was registered with ClinicalTrials.gov (NCT02221622). All participants provided written informed consent prior to participation.

All individuals were initially included in these exploratory analyses. However, one individual was excluded from the hippocampal analyses due to a missing T1-weighted image, two individuals were excluded from the rs-fMRI analyses and two individuals were excluded from the DWI analyses for incomplete imaging datasets ($n = 1$) or poor quality at one or both imaging sessions ($n = 1$). Demographic characteristics are presented in Table 1.

2.2 | Image acquisition and processing

All participants completed a multimodal neuroimaging battery prior to treatment and at week 16.

Imaging data were collected on a 3.0 Tesla GE Signa HDxt MRI scanner at USC. The imaging protocol is described in Supplement 1. Anatomical, rs-fMRI, and DWI data were pre-processed separately using Freesurfer,[31] fMRIPrep,[32] and QSIPrep.[33] Functional connectivity and regional homogeneity (ReHo) from pre-processed rs-fMRI data were calculated using the eXtensible Connectivity Pipeline (XCP Engine, v. 1.2.3). White matter microstructural integrity was quantified using both fractional anisotropy (FA) and QA in DSI Studio (March 11, 2021 release) using the pre-processed DWI data. All processing pipelines are described in Supplement 1.

HIGHLIGHTS

- Allopregnanolone (ALLO), a regenerative therapeutic, has the potential to alter disease progression and regenerate the brain in Alzheimer's disease (AD).
- The greatest effects of ALLO on hippocampal volume were seen in apolipoprotein E (*APOE*) ε4 carriers.
- White matter integrity and connectivity were preserved in ALLO-treated participants.
- ALLO strengthened local, inter-regional, and network-level functional connectivity.
- Exploratory outcomes support the use of imaging endpoints in a phase 2 clinical trial to advance the development of ALLO as a regenerative therapeutic in persons with mild AD.

RESEARCH IN CONTEXT

1. Systematic Review: Allopregnanolone (ALLO) promoted neurogenesis and oligogenesis and recovered cognitive function in preclinical Alzheimer's disease (AD) models. Considerable evidence supports ALLO's safety and regenerative capabilities. However, to date, there is limited neuroimaging evidence of ALLO's effects in humans.
2. Interpretation: ALLO was associated with increased hippocampal volume in a subset of participants, particularly *APOE* ε4 carriers. White matter integrity and connectivity was preserved and functional connectivity at multiple scales (local, inter-regional, network-wise) was strengthened in ALLO recipients. Our findings are consistent with published preclinical translational data demonstrating ALLO's neuro-regenerative capabilities.
3. Future Directions: Neuroimaging evidence of regeneration supported advancement of ALLO to a phase 2 proof-of-concept efficacy clinical trial.

2.3 | Statistical analyses

The emphasis for all exploratory statistical analyses was to present conservative estimates of potential effects of ALLO on brain structure and function. To this end, we report effect-size estimates and confidence intervals. Where relevant, we include *P*-value estimates for parity with similar studies; however, *P*-values should be interpreted only as indicators of avenues for further exploration.

2.3.1 | Hippocampal volume

Change from baseline ([Follow up—Baseline]/Baseline) was computed for the left and right hippocampi. Change from baseline outcomes included left and right hippocampal volumes segregated by sex (males vs females), *APOE* genotype (*APOE* ε3/ε3 carriers vs *APOE* ε4 carriers), and dose (placebo, 2, 4, 6 mg+). We previously reported no statistically significant changes in hippocampal volumes using one-way baseline-adjusted analyses of covariance (ANCOVAs) on change values.[12] Therefore, and given the small *n* of each subgroup within each treatment group, these data are presented and discussed qualitatively without specific statistical analyses.

2.3.2 | Whole-brain tractography

DWI preprocessing details are detailed in Supplement 1. Using the preprocessed DWI images, diffusion MRI connectometry[34] was used to derive correlational tractography demonstrating longitudinal changes (post-treatment—baseline) in both FA and QA associated with treatment group assignment (1 = ALLO, -1 = Placebo). A non-parametric Spearman correlation was used to derive the correlation. A total of 22 subjects were included in each analysis. A T-score threshold of 2.5 was assigned and tracked using a deterministic fiber tracking algorithm[35] to obtain correlational tractography. The tracks were filtered by topology-informed pruning[36] with four iteration(s). A length threshold of 20 mm was used to select tracks. To estimate the false-discovery rate (FDR), a total of 4000 randomized permutations were applied to the treatment group label to obtain the null distribution of the track length.

2.3.3 | Functional connectivity

Resting-state fMRI pre-processing steps and estimation of atlas-based functional connectivity are described in detail in Supplement 1. For each region of interest (ROI) to ROI connection in the functional connectivity matrices (edges) as well as ROI-specific ReHo, we performed a two-step linear regression to remove motion effects from each session separately, extract the residuals, and then to further residualize the post-treatment residuals on the baseline residuals. This yielded baseline-adjusted post-treatment estimates. We analyzed the baseline-adjusted edge-wise and ROI-wise ReHo data using DABEST (v. 0.3.1;[37]) to estimate between-group effect sizes (Hedges' *g*), 95% bias-corrected, accelerated (BCa) confidence intervals (20,000 bootstrap resamples), and empirical *P*-values (5000 permutations).

In addition to the edge-wise analyses, network-level changes in functional connectivity were computed. Each of the 473 ROIs was assigned to one of 11 networks, which included 9 cortical networks,[38] a subcortical network, and a cerebellar network resulting in both within-network (eg, limbic network) and cross-network (eg, default mode—visual network) connections. Within-network connectivity and cross-network connectivity values were computed as a weighted mean of the associated edge weights,[39] resulting in 11 within-network and 55 cross-network connectivity values. Post-treatment connectivity was regressed on baseline connectivity per network and analyzed with DABEST as described above.

For edge-wise, network-wise, and ROI-wise analyses, only those between-group differences whose effect size BCa confidence intervals did not include 0 were retained. FDR-adjusted empirical *P*-values were then computed.

3 | RESULTS

3.1 | Hippocampal volume

Prior to treatment, there were no between-group differences in left ($t_{13.091} = 0.925$, $P = .372$) (Figure 1A) or right hippocampal volumes ($t_{11.525} = 0.539$, $P = .600$) (Figure 1B), which was consistent whether groups were evaluated as a whole or when stratified by APIOE ε4 allele. Details of hippocampal volumes and change rates are summarized in Figure 1 and Table 2.

Placebo was associated with 0% gain and up to a 15% loss in left hippocampal volume (Figure 1C) and 7% loss in right hippocampal volume (Figure 1D). ALLO was associated with changes from baseline ranging from 7% gain to 10% loss in the left hippocampus (Figure 1C) and 7% gain to 7% loss in the right hippocampus (Figure 1D). No discernible sex-dependent effects were observed for either group (Figure 1E–F). An *APOE* genotype effect was observed where ALLO-treated *APOE* ε4 carriers exhibited the greatest gains in left and right hippocampal volume compared to non-carriers (Figure 1G–H).

Consistent with our prior report,[12] the optimal ALLO dose (4 mg) was associated with up to 7% gain and 5% loss across both the left and right hippocampi (Figure 1I–J). It is important to note that no ALLO dose was associated with the maximum loss observed in the placebo group. Furthermore, placebo administration was not associated with the maximal gain observed in any of the ALLO doses (Figure 1I–J).

3.2 | Whole-brain tractography

A total of 690 tracts localized in the right superior corticostriatal tract, bilateral cerebellum, and left superior longitudinal fasciculus (Figure 2A) exhibited between-group differences when FA formed the local connectome fingerprints (Figure 2A–C). In 100% of these tracts, individuals receiving ALLO exhibited increased FA, whereas individuals in the placebo group exhibited decreased FA (Figure 2B). Furthermore, a total of 1888 tracts (Figure 2D) exhibited statistically significant between-group differences (FDR corrected $P < .05$) when QA was used to form local connectome fingerprints. ALLO-treated participants, all doses combined, exhibited sustained QA in 1487 of 1888 tracts or 78.23% of the total (FDR corrected $P < .017$) (Figure 2D–F; red tracts),

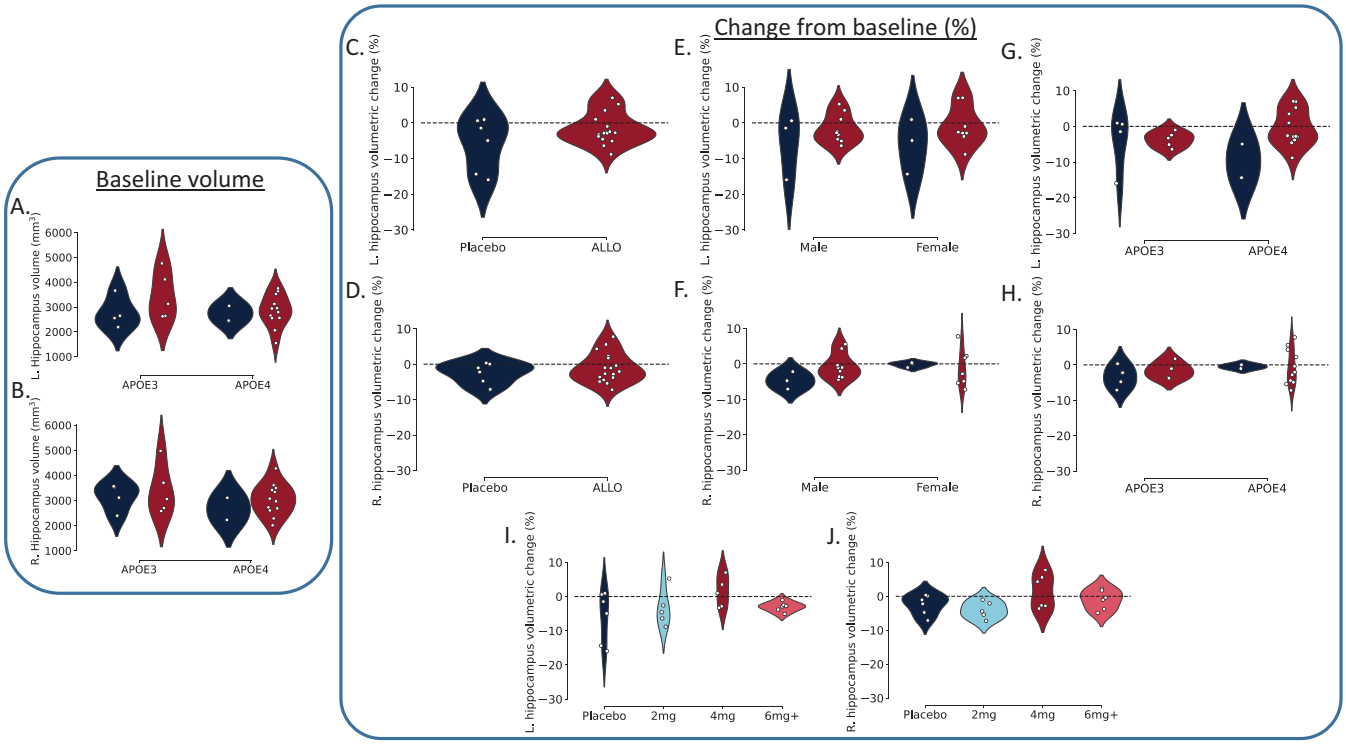

FIGURE 1 Impact of allopregnanolone (ALLO) on hippocampal volumes across sex, apolipoprotein E (*APOE*) genotype, and dose. Baseline hippocampal volumes for the left (A) and right (B) hippocampi stratified by *APOE* allele and intervention group (placebo, ALLO). After 12 weeks of allopregnanolone or placebo treatment, change was computed as (Follow up—Baseline/Baseline * 100). Differences are reported for placebo versus ALLO overall (C–D) as well as stratified by sex (E–F), genotype (G–H), and for each dosing level of ALLO (I–J). The 4 mg dose of ALLO was associated with the greatest gains in both left (I) and right (J) hippocampal volume. All gains were observed in *APOE* ε4 carriers, ranging from 0.6% to 7.8% increases in volume

which included tracts in the body of the corpus callosum, right posterior thalamic radiation, and left superior corticostriatal tract. In comparison, individuals in the placebo group exhibited greater increase in QA in 21.77% of the statistically significant tracts ($n = 411$ tracts; FDR corrected $P < .046$) (Figure 2D–E, 2G; blue tracts), primarily in the superior cerebellar peduncle, left superior corticostriatal tract, and cranial nerves III and VII.

3.3 | Inter-regional functional connectivity

After controlling for baseline edge-wise functional connectivity, a total of 726 edges out of 111,628 (0.65%) possible connections exhibited large differences between the ALLO and placebo groups ($|g| > 1.35$ for all edges) where confidence intervals did not include 0 and survived multiple comparisons correction at an FDR corrected $P < .05$. This included 491 edges with greater and 235 edges with lower connectivity values in the ALLO-treated group. A total of 32 edges survived multiple comparisons correction at a more stringent FDR-corrected $P < .01$ ($|g| > 1.80$ for all edges) (Figure 3A-D). Among these, 25 edges had greater connectivity and 7 edges had lower connectivity in the ALLO group after treatment when controlling for baseline edge-wise functional connectivity.

3.4 | Network-wise functional connectivity

At baseline, mean network-wise functional connectivity values ranged from −0.0908 to 0.0624 in the placebo group (Figure 3E upper panel) and from −0.0234 to 0.0340 in the ALLO group (Figure 3E lower panel). Following 12 weeks on placebo, connectivity decreased in the majority of network pairs (Figure 3F upper panel) while remaining unchanged or increasing in the ALLO group (Figure 3F lower panel). After adjusting for baseline connectivity, the ALLO treatment group exhibited greater connectivity in three cross-network pairs compared to placebo (Hedges $g > 1.16$; all FDR $P \leq .026$) (Figure 3G), which included greater connectivity between the limbic somatomotor networks, between the limbic and cerebellar networks, and between the limbic and DMNs (Figure 3G). Compared to placebo, the ALLO group exhibited lower connectivity between the cerebellum and subcortical gray matter (Hedges $g = 1.17$; FDR corrected $P = .024$; Figure 3G).

3.5 | Intra-regional functional connectivity

Following the 12-week treatment period, 29 regions (out of 473) exhibited large between-group differences, with effect sizes ranging from |0.74 | < to < |1.36| Hedges' g (Figure 3H). For these 29 regions, 95%

TABLE 2 Baseline hippocampal volumes, absolute and relative change by group

	Placebo ($n = 6$)		ALLO ($n = 17$)	
	L. hippocampus	R. hippocampus	L. hippocampus	R. hippocampus
Baseline (mm^3)	2759.20 ± 213.87	2992.30 ± 230.12	3021.22 ± 186.08	3149.41 ± 178.53
Change (mm^3)	−148.82 ± 77.96 [−407.3, 33.8]	−74.32 ± 40.73 [−254.0, 12.2]	−44.99 ± 29.69 [−181.8, 194.1]	−34.13 ± 29.38 [−179.9, 230.7]
Change (%)	−5.87 ± 3.07 [−15.95, 0.92]	−2.45 ± 1.20 [−7.12, 0.35]	−1.35 ± 1.11 [−8.82, 7.02]	−1.04 ± 1.00 [−7.22, 7.77]
Change by sex (mm^3)				
Male	−141.17 ± 133.79 [−407.3, 16.0]	−145.53 ± 55.81 [−254.0, -68.5]	−55.27 ± 42.51 [−168.7, 191.2]	−34.02 ± 37.50 [−179.9, 145.6]
Female	−156.47 ± 111.49 [−352.3, 33.8]	−3.10 ± 10.46 [−23.1, 12.2]	−33.43 ± 43.85 [−181.8, 194.1]	−34.25 ± 48.83 [−163.9, 230.7]
Change by sex (%)[a]				
Male	−5.61 ± 5.21 [−15.95, 0.60]	−4.69 ± 1.42 [−7.12, -2.20]	−1.65 ± 1.34 [−6.39, 5.25]	−0.72 ± 1.17 [−4.44, 5.59]
Female	−6.13 ± 4.45 [−14.36, 0.92]	−0.21 ± 0.42 [−1.04, 0.35]	−1.00 ± 1.92 [−8.82, 7.02]	−1.41 ± 1.76 [−7.23, 7.77]
Change by APOE load (mm^3)				
APOE ε3/ε3	−97.43 ± 104.23 [−407.3, 33.8]	−106.10 ± 55.79 [−254.0, 12.2]	−118.18 ± 24.56 [−168.7, -31.5]	−58.18 ± 38.79 [−179.9, 53.3]
APOE ε4+	−251.60 ± 100.70 [−352.30, -150.9]	−10.75 ± 12.35 [−23.1, 1.6]	−14.49 ± 37.92 [−181.8, 194.1]	−24.11 ± 38.98 [−163.9, 230.7]
Change by APOE load (%)[a]				
APOE ε3/ε3	−3.97 ± 4.03 [−15.95, 0.92]	−3.43 ± 1.61 [−7.12, 0.35]	−3.65 ± 0.95 [−6.39, -1.01]	−1.55 ± 1.01 [−3.78, 1.74]
APOE ε4+	−9.66 ± 4.70 [−14.36, -4.95]	−0.49 ± 0.54 [−1.04, 0.05]	−0.39 ± 1.46 [−8.82, 7.02]	−0.83 ± 1.38 [−7.22, 7.77]

Note: Values are listed as mean ± SE; minimum and maximum values are included in square brackets.
[a]Percent change relative to baseline volume.

confidence intervals did not include 0, with FDR corrected *P*-values ranging from 0.082 ≤ to ≤0.122. Compared to the ALLO group, the placebo group exhibited greater ReHo in nine ROIs (31% of the regions with large between-group differences; Figure 3H) after accounting for baseline values, including areas associated with bilateral somatomotor networks and dorsal attention networks (Figure 3C). Compared to the placebo group, the ALLO-treated groups combined exhibited greater ReHo after accounting for baseline values in 20 ROIs (69% of the regions with large between-group differences; Figure 3H), including areas of the posterior cingulate, somotamotor cortex, prefrontal cortex, and precuneus. Specified regions are included in Table S1.

4 | DISCUSSION

The primary purpose of these analyses was to investigate exploratory endpoints for future clinical trials of ALLO for the treatment of AD. ALLO treatment was associated with increased left and right hippocampal volume in some individuals with early AD, which was most apparent in the 4 mg dose group. Indicators of greater white matter integrity occurred in hundreds of fiber tracts. In parallel, individuals treated with ALLO exhibited increased functional connectivity, both in ROI-to-ROI connectivity and mean network connectivity. These results support a potential regenerative effect of ALLO on measures of hippocampal structure, white matter integrity, and functional connectivity.

4.1 | Hippocampal volume

We hypothesized that if ALLO targets the regenerative niche of the hippocampus,[4–8] then regeneration would be evident as either increased hippocampal volume relative to participant baseline or to placebo-treated participants, or decreased magnitude of hippocampal atrophy relative to participant baseline or to placebo. Analyses conservatively suggest a numerical trend toward decreased atrophy in ALLO-treated participants across all doses, with the greatest potential for regeneration in the 4 mg dose group. It is notable that all potentially beneficial effects were observed in *APOE ε4* carriers, with some *APOE ε4* carriers receiving ALLO exhibiting volumetric increases

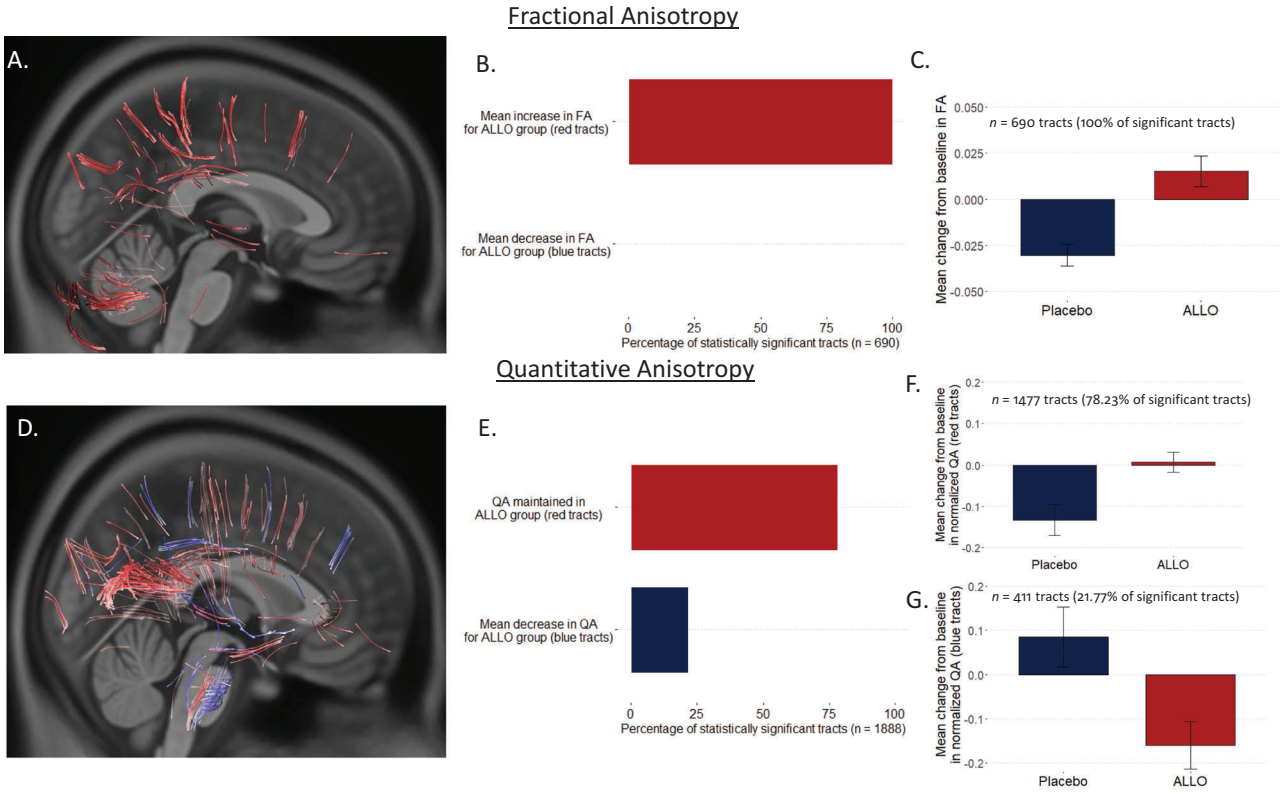

FIGURE 2 Impact of allopregnanolone (ALLO) on white matter integrity. Fractional anisotropy (FA; A–C) and quantitative anisotropy (QA; D–G) were used to create local connectome footprints to track white matter changes following treatment. Using FA, a total of 690 tracts survived multiple comparisons correction (false-discovery rate [FDR] corrected $P < .004$)(A), with 100% of these tracts (B) showing a mean increase in FA for the ALLO group compared to the placebo group (C). Using QA, a total of 1888 tracts survived multiple comparisons correction (D); 78.32% of these tracts (D red-colored tracts; E–F) showed no change in QA for participants receiving ALLO compared to placebo, whereas 21.77% of the tracts (D blue-colored tracts; E, G) showed decreased QA in ALLO participants compared to placebo

ranging from 0.6% to 7.8%. Of these, 42% had increased left hippocampal volume and 33% had increased right hippocampal volume, whereas neither of the *APOE* ε4 carriers in the placebo group demonstrated increased hippocampal volume. Positive volumetric change was not seen in *APOE* ε3 participants, suggesting that *APOE* ε4 carriers are a potential responder subgroup. The effect of the *APOE* ε4 allele on hippocampal structure has been noted previously, with greater hippocampal atrophy in *APOE* ε4 carriers and left-hemispheric atrophy greater than the right.[40–42]

Important for analyses reported herein, significant hippocampal loss can be detected within a 6-month window in early AD, which is accelerated in the presence of the *APOE* ε4 allele.[20] Placebo *APOE* ε4 carriers exhibited a -9.7% change over 3 months, whereas ALLO-treated participants exhibited a -1.35% (left) to -1.04% (right) change in hippocampal volume over the same time period (Table 2). This rate of change in the ALLO-treated *APOE* ε4 carriers was less than the volume loss reported for mild cognitive impairment (MCI) and AD patients (-2% to -3.3%) over 6 months.[20] Of interest, the impact of ALLO percent change in volume loss from baseline in ALLO-treated *APOE* ε4 carriers was most apparent in the left hippocampus, which exhibited a -0.4% change compared to the placebo *APOE* ε4 carriers, which showed a -9.7% change over 3 months.

4.2 | White matter integrity

Because ALLO promoted white matter remyelination[4] and oligodendrogenesis in animal models of AD,[8] we hypothesized that if ALLO exerted a regenerative effect on white matter, such effects would be detectable via diffusion-weighted MRI. Here we used two diffusion metrics: FA and QA. Generally, FA is indicative of white matter integrity[43,44] whereas QA indicates connectivity.[34,45]

A total of 690 and 1888 tracts exhibited baseline to post-treatment changes that differed between the ALLO and placebo groups for FA and QA, respectively. ALLO treatment was associated with increased (100% of tracts identified for FA) or maintained (78.23% of fibers identified for QA) diffusion characteristics, primarily in the corpus callosum, corticostriatal, longitudinal, cerebellar, and thalamic radiation fibers. This combination of improved FA based integrity and maintained QA based connectivity of fibers in the ALLO-treated group is indicative of sustained structural connectivity.[35,45] In contrast, the placebo group exhibited a decrease in both FA and QA for these same fibers, which may reflect axonal loss or demyelination resulting in more isotropic diffusion (decreased FA) and decreased structural connectivity (decreased QA).[45]

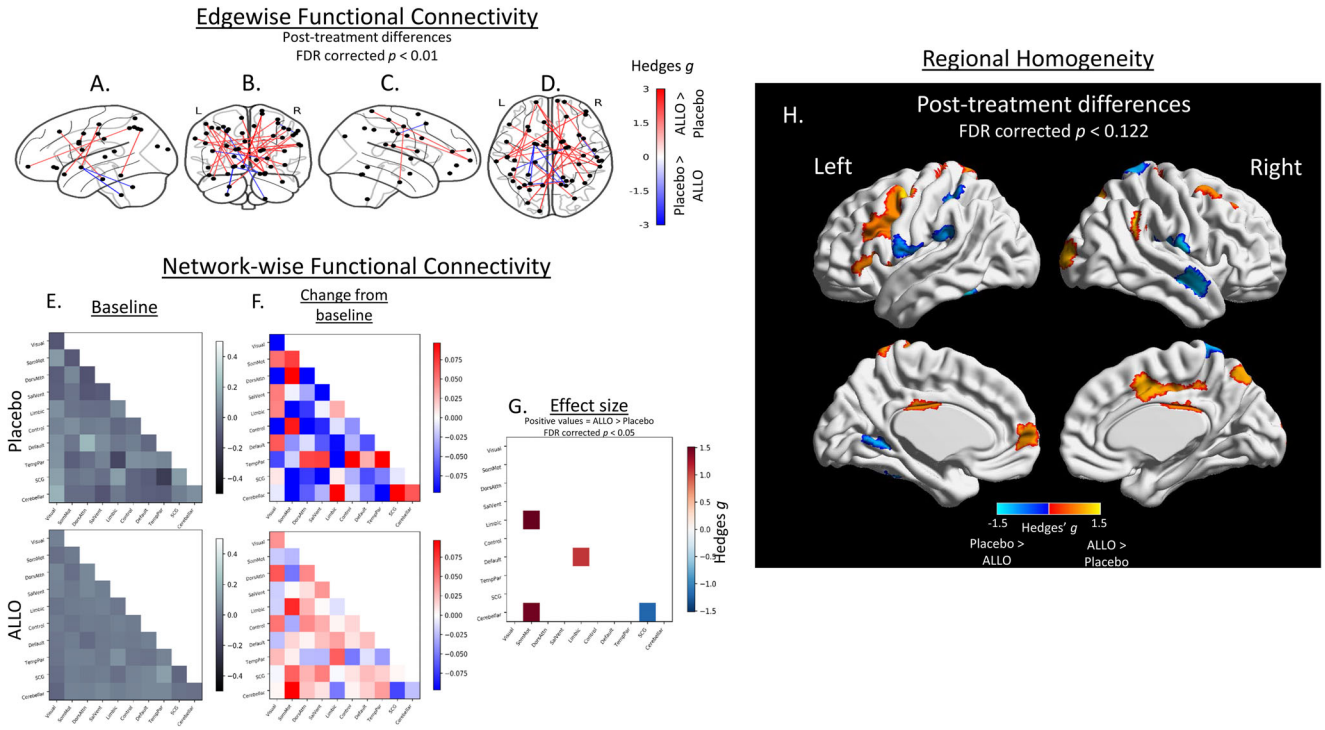

FIGURE 3 Impact of allopregnanolone (ALLO) on inter- and intra-regional functional connectivity. Post-treatment group-wise differences in functional connectivity were evaluated at a region-to-region ("edge-wise") (A–D), network-wise (E–G), and within-region ("Regional Homogeneity") (H) level using an atlas-based approach ($n = 473$ total regions) and are reported as Hedges' g effect sizes. A total of 32 edges exhibited large ($|g| > 1.80$; false-discovery rate (FDR)–corrected $P < .01$) differences, with 25 edges exhibiting greater connectivity in the ALLO group. These edge-wise connections are overlaid on the left hemisphere surface (A), a coronal view (B), the right hemisphere surface (C), and an axial view (D). These regions were additionally assigned to one of 11 large-scale networks (E). Simple differences from baseline (E) to post-treatment in network-wise functional revealed general patterns of decrease in the placebo group (F, top) and limited changes or increases in the ALLO group (F, bottom). Baseline-adjusted network models revealed larger increases in cross-network functional connectivity between the limbic network and both the default mode and somatomotor networks, and decreases in cerebellar-subcortical gray matter in the ALLO group compared to the placebo group ($|g| > 1.16$; FDR corrected $P < .05$)(G). Finally, ALLO was associated with larger increases ($g > 0.74$) in regional homogeneity in a total of 20 regions, including the prefrontal, posterior cingulate, and precuneus regions, whereas larger increases ($g > 0.89$) in the placebo group were observed in nine regions, including those associated with the bilateral somatomotor and dorsal attention networks (H). These regions with large differences were significant at FDR corrected $.082 < P < .122$ level

One possible interpretation of the ALLO profile is neuroplastic changes within these fiber tracts. Past work has shown that both increases and decreases in QA without a change in FA can reflect local neuroplasticity,[46,47] particularly in the corpus callosum.[46] If ALLO is exerting a neurogenic effect on white matter,[4,8] then local neuroplastic changes may be reflected in this smaller subset of the overall identified fibers. Although the true magnitude of impact on white matter integrity following ALLO requires larger samples, these findings suggest that ALLO exerts protective or regenerative effects on white matter integrity and structural connectivity.

4.3 | Inter-regional functional connectivity

Large differences in both edge-wise and network-level functional connectivity between the ALLO and placebo groups were observed after controlling for pre-treatment connectivity. Notably, ALLO was associated with stronger functional connectivity between the limbic network and both the default mode and somatomotor networks. The limbic network includes the bilateral temporal poles and orbitofrontal cortex. Altered structural and functional connectivity of both the orbitofrontal cortex and the DMN is associated with AD.[26–28] Strengthened functional connectivity between these networks may facilitate cognitive improvements with longer treatment. In contrast, the placebo group exhibited more frequent reduced connectivity in network-level functional connectivity (Figure 3), whereas functional connectivity in the ALLO group was often increased or unchanged. Although the overall magnitude of differences between groups was not large, these findings are consistent with white matter integrity outcomes and suggest that ALLO may promote and or preserve within- and across-network connectivity.

4.4 | Intra-regional functional connectivity

Regional homogeneity quantifies local functional connectivity and is generally regarded as a measure of local functioning. Prior work indicates that ReHo is reduced in both the medial prefrontal

cortex and precuneus in the AD brain as well as in amnestic MCI.[48–50] In addition, lower ReHo values are associated with decreased cognitive performance.[48,49] In the ALLO-treated group, greater ReHo was observed in critical areas of the DMN, including prefrontal regions and the precuneus, compared to the placebo group. These regions are associated with the default mode network and, coupled with the observations regarding inter-regional functional connectivity, provide additional evidence indicating that ALLO may promote functional connectivity across DMN structures that could, in turn, facilitate preserved cognitive capability. Although none of the between-group differences survived multiple comparisons correct at the $P < .05$ level, all of the reported effect sizes were large ($|g| > 0.74$), had bootstrapped confidence intervals that excluded 0, and were significant at an FDR corrected $P < .122$ level, suggesting the possibility of effects in larger samples.

4.5 | Limitations

This phase 1b/2a clinical trial was powered to determine safety and establish maximally tolerated dose in the target AD population and thus not specifically powered for these exploratory outcomes. The small sample size is an important consideration in interpreting the present findings. AD patients generally exhibit a high degree of heterogeneity in imaging outcomes, and such heterogeneity is accentuated with small sample sizes. Where possible, we have endeavored to be conservative with our statistics and interpretations as well as to emphasize effect sizes particularly for the functional connectivity analyses, where a large number of tests were conducted. The purpose here was not to provide conclusive evidence of ALLO effect but rather to identify mechanistic and regenerative-relevant candidate endpoints for future trials and to determine target effect sizes on which to power such trials. The findings here support further investigation of ALLO on hippocampal atrophy, as well as white matter integrity and functional connectivity.

In addition, the rs-fMRI and DWI imaging sequences used for the present analyses were not fully optimized. The rs-fMRI acquisition was a single-band acquisition with a long repetition time (3 seconds). The DWI acquisition was acquired in two separate sequences (individual acquisitions for each shell) and had highly anisotropic voxel sizes. Furthermore, there were a low number ($n < 25$) directions per shell, limiting the use of potentially informative microstructural analyses available from multi-shell acquisitions, such as diffusion kurtosis imaging and neurite orientation dispersion and density imaging.

Despite the small sample size and imaging limitations, the consistency of the imaging biomarker results, both within and across modalities, provided the basis for designing a larger phase 2 trial specifically powered on imaging endpoints. Multiband acquisitions (rs-fMRI, DWI), sub-second repetition times (rs-fMRI), isotropic voxel sizes (rs-fMRI, DWI), and optimized multi-shell parameters (DWI) are already planned for this phase 2 trial.

5 | CONCLUSIONS

Analyses of exploratory imaging outcomes indicated that ALLO treatment for 12 weeks was associated with a numerical trend of decreased hippocampal atrophy with an increase in volume detected in some *APOE* ε4 carriers in both women and men. Specifically, we found that participants receiving ALLO had maintained or increased white matter integrity as well as generally increased local, inter-regional, and network level functional connectivity in regions and networks associated with cognitive performance and vulnerability in AD. These results support the use of MRI- based imaging outcomes to detect potential regenerative responses in the AD brain. To that end, the REGENBRAIN Phase 2 proof-of-concept trial of ALLO as regenerative therapeutic for *APOE* ε4–positive persons with mild AD is currently underway (NCT04838301).

ACKNOWLEDGMENTS

To all the study participants and their families, the authors extend deep gratitude for their commitment and dedication to the phase 1 clinical trial of allopregnanolone for Alzheimer's disease. They also acknowledge and appreciate the exceptional contributions of the University of California (USC) Alzheimer's Disease Research Center (ADRC) leadership, Helena Chui, and staff; members of the Brinton laboratory team including Ronald Irwin, Eliza Bacon, and Maunil Desai, for their valuable contribution to the clinical trial. This work was financially supported by grants from the National Institute on Aging (UF-1AG046148, U01-AG031115, U01-AG047222) and ADDF-20150701 to Roberta Diaz Brinton as well as P30-AG066530 to Lon Schneider (USC ADRC clinical core).

CONFLICT OF INTEREST

Adam C. Raikes reports no disclosures. Gerson D. Hernandez hold a leadership position with Neutherapeutics. Dawn C. Matthews is a paid consultant and CEO of ADM Diagnostics, Ana S. Lukic is VP of Research and Development for ADM Diagnostics, Meng Law reports no competing interests. Yonggang Shi reports no competing interests. Lon S. Schneider reports grants from Biogen, Roche/Genentech, Eli Lilly and Company, Novartis, and Biohaven; personal fees from Merck, Eli Lilly and Company, and Roche/Genentech for serving on the data and safety monitoring boards; personal fees from Takeda for serving as a consultant and on an adjudication committee; and consulting fees from AC Immune, Avraham Pharmaceuticals, Boehringer Ingelheim, Cognition Therapeutics, Cotexyme, Eisai, Neurim Pharmaceuticals, Neuronix, Tau RX, Toyama, Abbott, and vTv Therapeutics outside the submitted work. Robert D. Brinton holds a leadership position with Neutherapeutics; and patent US8969329B2 for allopregnanolone for the treatment of neurodegenerative diseases.

REFERENCES

1. Association As. 2020 Alzheimer's disease facts and figures. *Alzheimers Dement*. 2020;16(3):391-460.

2. Cummings J, Lee G, Ritter A, Sabbagh M, Zhong K. Alzheimer's disease drug development pipeline: 2020. *Alzheimers Dement (N Y)*. 2020;6(1):e12050.
3. Brinton RD. Neurosteroids as regenerative agents in the brain: therapeutic implications. *Nat Rev Endocrinol*. 2013;9(4):241-250.
4. Chen S, Wang JM, Irwin RW, Yao J, Liu L, Brinton RD. Allopregnanolone promotes regeneration and reduces β-amyloid burden in a preclinical model of Alzheimer's disease. *PLoS One*. 2011;6(8):e24293.
5. Singh C, Liu L, Wang JM, et al. Allopregnanolone restores hippocampal-dependent learning and memory and neural progenitor survival in aging 3xTgAD and nonTg mice. *Neurobiol Aging*. 2012;33(8):1493-1506.
6. Wang JM, Singh C, Liu L, et al. Allopregnanolone reverses neurogenic and cognitive deficits in mouse model of Alzheimer's disease. *Proc Natl Acad Sci*. 2010;107(14):6498-6503.
7. Wang JM, Johnston PB, Ball BG, Brinton RD. The neurosteroid allopregnanolone promotes proliferation of rodent and humanneural progenitor cells and regulates cell-cycle gene and protein expression. *J Neurosci*. 2005;25(19):4706-4718.
8. Chen S, Wang T, Yao J, Brinton RD. Allopregnanolone promotes neuronal and oligodendrocyte differentiation in vitro and in vivo: therapeutic implication for Alzheimer's disease. *Neurotherapeutics*. 2020;17(4):1813-1824.
9. De Nicola AF, Meyer M, Garay L, et al. Progesterone and allopregnanolone neuroprotective effects in the wobbler mouse model of amyotrophic lateral sclerosis. *Cell Mol Neurobiol*. 2021;42(1):23-40.
10. Diviccaro S, Cioffi L, Falvo E, Giatti S, Melcangi RC. Allopregnanolone: an overview on its synthesis and effects. *J Neuroendocrinol*. 2021:e12996. https://doi.org/10.1111/jne.12996.
11. Irwin RW, Solinsky CM, Loya CM, et al. Allopregnanolone preclinical acute pharmacokinetic and pharmacodynamic studies to predict tolerability and efficacy for Alzheimer's disease. *PLoS One*. 2015;10(6):e0128313.
12. Hernandez GD, Solinsky CM, Mack WJ, et al. Safety, tolerability, and pharmacokinetics of allopregnanolone as a regenerative therapeutic for Alzheimer's disease: a single and multiple ascending dose phase 1b/2a clinical trial. *Alzheimers Dement (N Y)*. 2020;6(1):e12107.
13. Irwin RW, Brinton RD. Allopregnanolone as regenerative therapeutic for Alzheimer's disease: translational development and clinical promise. *Prog Neurobiol*. 2014;113:40-55.
14. Irwin RW, Solinsky CM, Brinton RD. Frontiers in therapeutic development of allopregnanolone for Alzheimer's disease and other neurological disorders. *Front Cell Neurosci*. 2014;8:203.
15. Irwin RW, Wang JM, Chen S, Brinton RD, Neuroregenerative mechanisms of allopregnanolone in Alzheimer's disease. *Front Endocrinol (Lausanne)*. 2011;2:117.
16. Parnetti L, Chipi E, Salvadori N, D'Andrea K, Eusebi P. Prevalence and risk of progression of preclinical Alzheimer's disease stages: a systematic review and meta-analysis. *Alzheimers Res Ther*. 2019;11(1):7.
17. Ferreira D, Nordberg A, Westman E. Biological subtypes of Alzheimer disease: a systematic review and meta-analysis. *Neurology*. 2020;94(10):436-448.
18. Dubois B, Villain N, Frisoni GB, et al. Clinical diagnosis of Alzheimer's disease: recommendations of the International Working Group. *Lancet Neurol*. 2021;20(6):484-496.
19. Rice L, Bisdas S. The diagnostic value of FDG and amyloid PET in Alzheimer's disease-A systematic review. *Eur J Radiol*. 2017;94:16-24.
20. Schuff N, Woerner N, Boreta L, et al. MRI of hippocampal volume loss in early Alzheimer's disease in relation to ApoE genotype and biomarkers. *Brain*. 2009;132(4):1067-1077.
21. Dallaire-Theroux C, Callahan BL, Potvin O, Saikali S, Duchesne S. Radiological-Pathological correlation in Alzheimer's disease: systematic review of antemortem magnetic resonance imaging findings. *J Alzheimers Dis*. 2017;57(2):575-601.
22. Hill DLG, Schwarz AJ, Isaac M, et al. Coalition Against Major Diseases/European Medicines Agency biomarker qualification of hippocampal volume for enrichment of clinical trials in predementia stages of Alzheimer's disease. *Alzheimers Dement*. 2014;10(4):421-429.
23. Arnerić SP, Kern VD, Stephenson DT. Regulatory-accepted drug development tools are needed to accelerate innovative CNS disease treatments. *Biochem Pharmacol*. 2018;151:291-306.
24. Harrison JR, Bhatia S, Tan ZX, et al. Imaging Alzheimer's genetic risk using diffusion MRI: a systematic review. *NeuroImage: Clinical*. 2020;27:102359.
25. Badhwar A, Tam A, Dansereau C, Orban P, Hoffstaedter F, Bellec P. Resting-state network dysfunction in Alzheimer's disease: a systematic review and meta-analysis. *Alzheimers Dement (Amst)*. 2017;8:73-85. doi:10/ggh86n.
26. Dennis EL, Thompson PM. Functional brain connectivity using fMRI in aging and Alzheimer's disease. *Neuropsychol Rev*. 2014;24(1):49-62.
27. Greicius MD, Srivastava G, Reiss AL, Menon V. Default-mode network activity distinguishes Alzheimer's disease from healthy aging: evidence from functional MRI. *Proc Natl Acad Sci U S A*. 2004;101(13):4637-4642.
28. Zhao T, Quan M, Jia J. Functional connectivity of default mode network subsystems in the presymptomatic stage of autosomal dominant Alzheimer's disease. *J Alzheimers Dis*. 2020;73(4):1435-1444.
29. Sole-Padulles C, Bartres-Faz D, Llado A, et al. Donepezil treatment stabilizes functional connectivity during resting state and brain activity during memory encoding in Alzheimer's disease. *J Clin Psychopharmacol*. 2013;33(2):199-205.
30. Li W, Antuono PG, Xie C, et al. Changes in regional cerebral blood flow and functional connectivity in the cholinergic pathway associated with cognitive performance in subjects with mild Alzheimer's disease after 12-week donepezil treatment. *Neuroimage*. 2012;60(2):1083-1091.
31. Reuter M, Schmansky NJ, Rosas HD, Fischl B. Within-subject template estimation for unbiased longitudinal image analysis. *Neuroimage*. 2012;61(4):1402-1418.
32. Esteban O, Markiewicz CJ, Blair RW, et al. fMRIPrep: a robust preprocessing pipeline for functional MRI. *Nat Methods*. 2019;16(1):111.
33. Cieslak M, Cook PA, He X, et al. QSIPrep: an integrative platform for preprocessing and reconstructing diffusion MRI data. *Nat Methods*. 2021;18(7):775-778.
34. Yeh F-C, Badre D, Verstynen T. Connectometry: a statistical approach harnessing the analytical potential of the local connectome. *Neuroimage*. 2016;125:162-171.
35. Yeh F-C, Verstynen TD, Wang Y, Fernández-Miranda JC, Tseng W-YI. Deterministic diffusion fiber tracking improved by quantitative anisotropy. *PLoS One*. 2013;8(11):e80713.
36. Yeh F-C, Panesar S, Barrios J, et al. Automatic removal of false connections in diffusion MRI tractography using topology-informed pruning (TIP). *Neurotherapeutics*. 2019;16(1):52-58.
37. Ho J, Tumkaya T, Aryal S, Choi H, Claridge-Chang A. Moving beyond P values: data analysis with estimation graphics. *Nat Methods*. 2019;16(7):565-566.
38. Yeo BTT, Krienen FM, Sepulcre J, et al. The organization of the human cerebral cortex estimated by intrinsic functional connectivity. *J Neurophysiol*. 2011;106(3):1125-1165.
39. Xia CH, Ma Z, Cui Z, et al. Multi-scale network regression for brain-phenotype associations. *Hum Brain Mapp*. 2020;41(10):2553-2566.
40. Pievani M, Galluzzi S, Thompson PM, Rasser PE, Bonetti M, Frisoni GB. APOE4 is associated with greater atrophy of the hippocampal formation in Alzheimer's disease. *Neuroimage*. 2011;55(3):909-919.
41. Li B, Shi J, Gutman BA, et al. Influence of APOE genotype on hippocampal atrophy over time - An N = 1925 surface-based ADNI study. *PLoS One*. 2016;11(4):e0152901.
42. Shi J, Leporé N, Gutman BA, et al. Genetic influence of apolipoprotein E4 genotype on hippocampal morphometry: an N = 725 surface-based

Alzheimer's disease neuroimaging initiative study. *Hum Brain Mapp*. 2014;35(8):3903-3918.
43. Song S-K, Sun S-W, Ramsbottom MJ, Chang C, Russell J, Cross AH. Dysmyelination revealed through MRI as increased radial (but unchanged axial) diffusion of water. *Neuroimage*. 2002;17(3):1429-1436.
44. Song S-K, Sun S-W, Ju W-K, Lin S-J, Cross AH, Neufeld AH. Diffusion tensor imaging detects and differentiates axon and myelin degeneration in mouse optic nerve after retinal ischemia. *Neuroimage*. 2003;20(3):1714-1722.
45. Yeh F-C, Vettel JM, Singh A, et al. Quantifying differences and similarities in whole-brain white matter architecture using local connectome fingerprints. *PLoS Comput Biol*. 2016;12(11):e1005203.
46. Yeh FC, Vettel JM, Singh A, et al. Quantifying differences and similarities in whole-brain white matter architecture using local connectome fingerprints. *PLoS Comput Biol*. 2016;12(11):e1005203.
47. Shen CY, Tyan YS, Kuo LW, Wu CW, Weng JC. Quantitative evaluation of rabbit brain injury after cerebral hemisphere radiation exposure using generalized q-sampling imaging. *PLoS One*. 2015;10(7):e0133001.
48. Zhang Z, Liu Y, Jiang T, et al. Altered spontaneous activity in Alzheimer's disease and mild cognitive impairment revealed by regional homogeneity. *Neuroimage*. 2012;59(2):1429-1440.
49. He Y, Wang L, Zang Y, et al. Regional coherence changes in the early stages of Alzheimer's disease: a combined structural and resting-state functional MRI study. *Neuroimage*. 2007;35(2):488-500.
50. Liu Y, Wang K, Yu C, et al. Regional homogeneity, functional connectivity and imaging markers of Alzheimer's disease: a review of resting-state fMRI studies. *Neuropsychologia*. 2008;46(6):1648-1656.

SUPPORTING INFORMATION

Additional supporting information may be found in the online version of the article at the publisher's website.

How to cite this article: Raikes AC, Hernandez GD, Matthews DC, et al. Exploratory imaging outcomes of a phase 1b/2a clinical trial of allopregnanolone as a regenerative therapeutic for Alzheimer's disease: Structural effects and functional connectivity outcomes. *Alzheimer's Dement*. 2022;8:e12258. https://doi.org/10.1002/trc2.12258